

**SYNTHESIS AND CHARACTERISATION OF NEW
Ru₃ AND Os₃ CLUSTERS WITH SULPHUR
CONTAINING PHOSPHINES, ALKYNE, AND
ANTIMONY LIGANDS**

HAFIZ MALIK HUSSIEN ABDELNASIR

UNIVERSITI SAINS MALAYSIA

2017

**SYNTHESIS AND CHARACTERISATION OF NEW
Ru₃ AND Os₃ CLUSTERS WITH SULPHUR
CONTAINING PHOSPHINES, ALKYNE, AND
ANTIMONY LIGANDS**

by

HAFIZ MALIK HUSSIEN ABDELNASIR

**Thesis submitted in fulfillment of the requirements
for the Degree of
Doctor of Philosophy**

June 2017

ACKNOWLEDGEMENT

Firstly, I would like to express my appreciation to my supervisor Prof Datuk Dr. Omar bin Shawkataly, for his constant encouragement, patience, guidance, inspiration, and support.

I am grateful to Dr. Imthyaz Ahmad Khan, for advice and encouragement during the study. Also, I wish to express gratitude to USM for fellowship and Postgraduate Research Grant Scheme (PRGS).

I would like to pass sincere respect to all the staffs of the School of Distance Education and School of Chemical Sciences for their providing facilities and assistances. Thankful to the technical staffs of the School of Chemical Sciences, USM, in particular, Mr Zahari Othman, Mr Mohd Radzly, and Mr Mohd Nizam. Thank the X-Ray Crystallography Unit of the School of Physics USM and X-Ray Crystallography Unit of the School of Chemistry UKM. Profoundly I am grateful to my colleagues for their help and moral support.

I am grateful to my mother and my late father. Favourable thank to my wife Siham for her constant support and strengthening. Finally, I thank my brothers, sisters, and my friends Ibrahim and Shadi for their financial support.

TABLE OF CONTENTS

ACKNOWLEDGEMENT	ii
TABLE OF CONTENTS	iii
LIST OF TABLES.....	ix
LIST OF FIGURES.....	xiii
LIST OF SCHEMES	xiii
LIST OF ABBREVIATIONS	xviii
ABSTRAK.....	xxv
ABSTRACT	xxviii
CHAPTER 1 – INTRODUCTION.....	1
1.1 Metal clusters chemistry.....	1
1.1.1 Triiron Dodecacarbonyl.....	3
1.1.2 Triruthenium dodecacarbonyl.....	3
1.1.3 Triosmium dodecacarbonyl.....	4
1.2 Ligands.....	5

1.2.1 Bidentate ligands (L-L) Types (P-P) and (As-As).....	5
1.2.2 Sulphur containing phosphines ligands.....	7
1.2.3 Alkyne ligands.....	8
1.2.4 Antimony ligands.....	9
1.2.5 Objectives.....	11
1.2.6 Scope of the present investigation.....	11
CHAPTER 2 - LITERATURE REVIEW	13
2.1 Carbonyl substitution.....	13
2.2 Bidentate ligands with Ru ₃ (CO) ₁₂	18
2.3 Sulphur containing phosphines ligands with Ru ₃ (CO) ₁₂ and Os ₃ (CO) ₁₂ ...	21
2.4 Alkyne ligands with Ru ₃ (CO) ₁₂	31
2.5 Antimony ligands with Ru ₃ (CO) ₁₂	44
2.5.1 Cytotoxicity of antimony compounds.....	47
CHAPTER 3 - EXPERIMENTAL	51
3.1 Synthesis of Ru ₃ and Os ₃ Clusters with P, S ligands	55
3.1.1 Synthesis of PPh ₂ C ₆ H ₄ SCH ₃	55
3.1.2 Synthesis of Ph ₂ PCH ₂ SPh.....	55

3.1.3	Synthesis of $[\text{Ru}_3(\text{CO})_{10}(\text{dpae})]$	56
3.1.4	Synthesis of $[\text{Ru}_3(\text{CO})_{11}(\text{PPh}_2\text{C}_6\text{H}_4\text{SCH}_3)]$	57
3.1.5	Synthesis of $[\text{Ru}_3(\text{CO})_9(\text{dppe})(\text{PPh}_2\text{C}_6\text{H}_4\text{SCH}_3)]$	58
3.1.6	Synthesis of $[\text{Ru}_3(\text{CO})_9(\text{dppm})(\text{PPh}_2\text{C}_6\text{H}_4\text{SCH}_3)]$	59
3.1.7	Synthesis of $[\text{Ru}_3(\text{CO})_9(\text{dpam})(\text{PPh}_2\text{C}_6\text{H}_4\text{SCH}_3)]$	59
3.1.8	Synthesis of $[\text{Ru}_3(\text{CO})_9(\text{dotpm})(\text{Ph}_2\text{PCH}_2\text{SPh})]$	60
3.1.9	Synthesis of $[\text{Os}_3(\text{CO})_{11}(\text{PPh}_2\text{C}_6\text{H}_4\text{SCH}_3)]$	61
3.1.10	Synthesis of $[\text{Os}_3(\text{CO})_{11}(\text{Ph}_2\text{PCH}_2\text{SPh})]$	62
3.1.11	Synthesis of $[\text{Os}_3(\text{CO})_{10}(\mu\text{-Ph}_2\text{PCH}_2\text{SPh})]$	62
3.2	Synthesis of Triruthenium clusters with alkyne ligands.....	64
3.2.1	Synthesis of $[\text{HRu}_3(\text{CO})_7(\text{dppm})(\text{C}_2(\text{C}_6\text{H}_4)\text{-4-OCH}_3)]$	64
3.2.2	Synthesis of $[\text{HRu}_3(\text{CO})_7(\text{dppe})(\text{C}_2\text{Si}(\text{CH}_3)_3)]$	65
3.2.3	Synthesis of $[\text{HRu}_3(\text{CO})_7(\text{dppe})(\text{C}_2(\text{C}_6\text{H}_4)\text{-4-OCH}_3)]$	65
3.2.4	Synthesis of $[\text{HRu}_3(\text{CO})_7(\text{dppf})(\text{C}_2\text{Si}(\text{CH}_3)_3)]$	66
3.2.5	Synthesis of $[\text{HRu}_3(\text{CO})_7(\text{dppf})(\text{C}_2(\text{C}_6\text{H}_4)\text{-4-OCH}_3)]$	67
3.2.6	Synthesis of $[\text{HRu}_3(\text{CO})_7(\text{dpae})(\text{C}_2\text{Si}(\text{CH}_3)_3)]$	68
3.2.7	Synthesis of $[\text{HRu}_3(\text{CO})_7(\text{dpae})(\text{C}_2(\text{C}_6\text{H}_4)\text{-4-OCH}_3)]$	69
3.2.8	Synthesis of $[\text{HRu}_3(\text{CO})_7(\text{dpam})(\text{C}_2(\text{C}(\text{CH}_3)_3)]$	69

3.2.9	Synthesis of $[\text{HRu}_3(\text{CO})_7(\text{dpam})(\text{C}_2(\text{C}_6\text{H}_4\text{-4-CH}_3))]$	70
3.2.10	Synthesis of $[\text{Ru}_3(\text{CO})_9(\text{dpam})(\text{COC}_6\text{H}_5)]$	71
3.3	Synthesis of Triruthenium carbonyl clusters with antimony ligands.....	73
3.3.1	Synthesis of $[\text{Sb}(\text{C}_6\text{H}_4\text{-3-OCH}_3)_3]$	73
3.3.2	Synthesis of $[\text{Sb}(\text{C}_6\text{H}_4)\text{SCH}_3)_3]\text{Cl}_2$	73
3.3.3	Synthesis of $[\text{Ru}_3(\text{CO})_{11}(\text{Sb}(\text{C}_6\text{H}_4\text{-3-OCH}_3)_3)]$	75
3.3.4	Synthesis of $[\text{Ru}_3(\text{CO})_9(\text{dppm})(\text{Sb}(\text{C}_6\text{H}_4\text{-3-OCH}_3)_3)]$	76
3.3.5	Synthesis of $[\text{Ru}_3(\text{CO})_9(\text{dpae})(\text{Sb}(\text{C}_6\text{H}_4\text{-3-OCH}_3)_3)]$	77
3.3.6	Synthesis of $[\text{Ru}_3(\text{CO})_{11}(\text{Sb}(\text{C}_{12}\text{H}_9)_3)]$	78
3.3.7	Synthesis of $[\text{Ru}_3(\text{CO})_9(\text{dppm})(\text{Sb}(\text{C}_{12}\text{H}_9)_3)]$	78
CHAPTER 4 - RESULTS AND DISCUSSIONS		80
4.1	Triruthenium and triosmium clusters with P, S ligands.....	80
4.1.1	Structure of $\text{PPh}_2\text{C}_6\text{H}_4\text{SCH}_3$ and $\text{Ph}_2\text{PCH}_2\text{SPh}$	80
4.1.2	Structure of $[\text{Ru}_3(\text{CO})_{10}(\text{dpae})]$	80
4.1.3	Structure of $[\text{Ru}_3(\text{CO})_{11}(\text{PPh}_2\text{C}_6\text{H}_4\text{SCH}_3)]$	88
4.1.4	Structure of $[\text{Ru}_3(\text{CO})_9(\text{dppe})(\text{PPh}_2\text{C}_6\text{H}_4\text{SCH}_3)]$	94
4.1.5	Structure of $[\text{Ru}_3(\text{CO})_9(\text{dppm})(\text{PPh}_2\text{C}_6\text{H}_4\text{SCH}_3)]$	100
4.1.6	Structure of $[\text{Ru}_3(\text{CO})_9(\text{dpam})(\text{PPh}_2\text{C}_6\text{H}_4\text{SCH}_3)]$	106

4.1.7	Structure of $[\text{Ru}_3(\text{CO})_9(\text{dotpm})(\text{Ph}_2\text{PCH}_2\text{SPh})]$	112
4.1.8	Structure of $[\text{Os}_3(\text{CO})_{11}(\text{PPh}_2\text{C}_6\text{H}_4\text{SCH}_3)]$	118
4.1.9	Structure of $[\text{Os}_3(\text{CO})_{11}(\text{Ph}_2\text{PCH}_2\text{SPh})]$	124
4.1.10	Structure of $[\text{Os}_3(\text{CO})_{10}(\mu\text{-Ph}_2\text{PCH}_2\text{SPh})]$	130
4.2	Triruthenium clusters with alkyne ligands.....	138
4.2.1	Structure of $[\text{HRu}_3(\text{CO})_7(\text{dppm})(\text{C}_2(\text{C}_6\text{H}_4)\text{-4-OCH}_3)]$	138
4.2.2	Structure of $[\text{HRu}_3(\text{CO})_7(\text{dppe})(\text{C}_2\text{Si}(\text{CH}_3)_3)]$	144
4.2.3	Structure of $[\text{HRu}_3(\text{CO})_7(\text{dppe})(\text{C}_2(\text{C}_6\text{H}_4)\text{-4-OCH}_3)]$	150
4.2.4	Structure of $[\text{HRu}_3(\text{CO})_7(\text{dppf})(\text{C}_2\text{Si}(\text{CH}_3)_3)]$	156
4.2.5	Structure of $[\text{HRu}_3(\text{CO})_7(\text{dppf})(\text{C}_2(\text{C}_6\text{H}_4)\text{-4-OCH}_3)]$	162
4.2.6	Structure of $[\text{HRu}_3(\text{CO})_7(\text{dpae})(\text{C}_2\text{Si}(\text{CH}_3)_3)]$	168
4.2.7	Structure of $[\text{HRu}_3(\text{CO})_7(\text{dpae})(\text{C}_2(\text{C}_6\text{H}_4)\text{-4-OCH}_3)]$	174
4.2.8	Structure of $[\text{HRu}_3(\text{CO})_7(\text{dpam})(\text{C}_2\text{C}(\text{CH}_3)_3)]$	180
4.2.9	Structure of $[\text{HRu}_3(\text{CO})_7(\text{dpam})(\text{C}_2(\text{C}_6\text{H}_4\text{-4-CH}_3)]$	186
4.2.10	Structure of $[\text{Ru}_3(\text{CO})_9(\text{dpam})(\text{COC}_6\text{H}_5)]$	192
4.3	Triruthenium carbonyl clusters with a new antimony ligands.....	199
4.3.1	Structure of $\text{Sb}(\text{C}_6\text{H}_4\text{-3-OCH}_3)_3$	199
4.3.2	Structure of $[\text{Sb}((\text{C}_6\text{H}_4)\text{SCH}_3)_3]\text{Cl}_2$	204

4.3.3	Structure of $[\text{Ru}_3(\text{CO})_{11}(\text{Sb}(\text{C}_6\text{H}_4\text{-3-OCH}_3)_3)]$	213
4.3.4	Structure of $[\text{Ru}_3(\text{CO})_9(\text{dppm})(\text{Sb}(\text{C}_6\text{H}_4\text{-3-OCH}_3)_3)]$	219
4.3.5	Structure of $[\text{Ru}_3(\text{CO})_9(\text{dpae})(\text{Sb}(\text{C}_6\text{H}_4\text{-3-OCH}_3)_3)]$	225
4.3.6	Structure of $[\text{Ru}_3(\text{CO})_{11}(\text{Sb}(\text{C}_{12}\text{H}_9)_3)]$	231
4.3.7	Structure of $[\text{Ru}_3(\text{CO})_9(\text{dppm})(\text{Sb}(\text{C}_{12}\text{H}_9)_3)]$	237
CHAPTER 5 - CONCLUSION		244
REFERENCES		248
APPENDICES		

LIST OF TABLES

		Page
Table 4.1	Crystal data and structure refinement for PPh ₂ C ₆ H ₄ SCH ₃ and Ph ₂ PCH ₂ SPh	85
Table 4.2	Selected bond lengths and angles for PPh ₂ C ₆ H ₄ SCH ₃ and Ph ₂ PCH ₂ SPh	86
Table 4.3	Crystal data and structure refinement for [Ru ₃ (CO) ₁₁ (PPh ₂ C ₆ H ₄ SCH ₃)]	91
Table 4.4	Selected Bond Lengths and Angles for [Ru ₃ (CO) ₁₁ (PPh ₂ C ₆ H ₄ SCH ₃)]	93
Table 4.5	Crystal data and structure refinement for [Ru ₃ (CO) ₉ (dppe)(PPh ₂ C ₆ H ₄ SCH ₃)]	97
Table 4.6	Selected Bond Lengths and Angles for [Ru ₃ (CO) ₉ (dppe)(PPh ₂ C ₆ H ₄ SCH ₃)]	99
Table 4.7	Crystal data and structure refinement for [Ru ₃ (CO) ₉ (dppm)(PPh ₂ C ₆ H ₄ SCH ₃)]	103
Table 4.8	Selected Bond Lengths and Angles for [Ru ₃ (CO) ₉ (dppm)(PPh ₂ C ₆ H ₄ SCH ₃)]	105
Table 4.9	Crystal data and structure refinement for [Ru ₃ (CO) ₉ (dpam)(PPh ₂ C ₆ H ₄ SCH ₃)]	109
Table 4.10	Selected Bond Lengths and Angles for [Ru ₃ (CO) ₉ (dpam)(PPh ₂ C ₆ H ₄ SCH ₃)]	111
Table 4.11	Crystal data and structure refinement for [Ru ₃ (CO) ₉ (dotpm)(PPh ₂ C ₆ H ₄ SCH ₃)]	115
Table 4.12	Selected Bond Lengths and Angles for [Ru ₃ (CO) ₉ (dotpm)(PPh ₂ C ₆ H ₄ SCH ₃)]	117
Table 4.13	Crystal data and structure refinement for [Os ₃ (CO) ₁₁ (PPh ₂ C ₆ H ₄ SCH ₃)]	121

Table 4.14	Selected Bond Lengths and Angles for $[\text{Os}_3(\text{CO})_{11}(\text{PPh}_2\text{C}_6\text{H}_4\text{SCH}_3)]$	123
Table 4.15	Crystal data and structure refinement for $[\text{Os}_3(\text{CO})_{11}(\text{Ph}_2\text{PCH}_2\text{SPh})]$	127
Table 4.16	Selected Bond Lengths and Angles for $[\text{Os}_3(\text{CO})_{11}(\text{Ph}_2\text{PCH}_2\text{SPh})]$	129
Table 4.17	Crystal data and structure refinement for $[\text{Os}_3(\text{CO})_{10}(\text{Ph}_2\text{PCH}_2\text{SPh})]$	133
Table 4.18	Selected Bond Lengths and Angles for $[\text{Os}_3(\text{CO})_{10}(\text{Ph}_2\text{PCH}_2\text{SPh})]$	135
Table 4.19	Spectroscopy data for Ru_3 clusters with sulphur containing phosphine ligands	136
Table 4.20	Crystal data and structure refinement for $[\text{HRu}_3(\text{CO})_7(\text{dppm})(\text{C}_2(\text{C}_6\text{H}_4)\text{-4-OCH}_3)]$	141
Table 4.21	Selected Bond Lengths and Angles for $[\text{HRu}_3(\text{CO})_7(\text{dppm})(\text{C}_2(\text{C}_6\text{H}_4)\text{-4-OCH}_3)]$	143
Table 4.22	Crystal data and structure refinement for $[\text{HRu}_3(\text{CO})_7(\text{dppe})(\text{C}_2\text{Si}(\text{CH}_3)_3)]$	147
Table 4.23	Selected Bond Lengths and Angles for $[\text{HRu}_3(\text{CO})_7(\text{dppe})(\text{C}_2\text{Si}(\text{CH}_3)_3)]$	149
Table 4.24	Crystal data and structure refinement for $[\text{HRu}_3(\text{CO})_7(\text{dppe})(\text{C}_2(\text{C}_6\text{H}_4)\text{-4-OCH}_3)]$	153
Table 4.25	Selected Bond Lengths and Angles for $[\text{HRu}_3(\text{CO})_7(\text{dppe})(\text{C}_2(\text{C}_6\text{H}_4)\text{-4-OCH}_3)]$	155
Table 4.26	Crystal data and structure refinement for $[\text{HRu}_3(\text{CO})_7(\text{dppf})(\text{C}_2\text{Si}(\text{CH}_3)_3)]$	159
Table 4.27	Selected Bond Lengths and Angles for $[\text{HRu}_3(\text{CO})_7(\text{dppf})(\text{C}_2\text{Si}(\text{CH}_3)_3)]$	161
Table 4.28	Crystal data and structure refinement for $[\text{HRu}_3(\text{CO})_7(\text{dppf})(\text{C}_2(\text{C}_6\text{H}_4)\text{-4-OCH}_3)]$	165

Table 4.29	Selected Bond Lengths and Angles for[HRu ₃ (CO) ₇ (dppf)(C ₂ (C ₆ H ₄)-4-OCH ₃)]	167
Table 4.30	Crystal data and structure refinement for [HRu ₃ (CO) ₇ (dpae)(C ₂ Si(CH ₃) ₃)]	171
Table 4.31	Selected Bond Lengths and Angles for [HRu ₃ (CO) ₇ (dpae)(C ₂ Si(CH ₃) ₃)]	173
Table 4.32	Crystal data and structure refinement for [HRu ₃ (CO) ₇ (dpae)(C ₂ (C ₆ H ₄)-4-OCH ₃)]	177
Table 4.33	Selected Bond Lengths and Angles for [HRu ₃ (CO) ₇ (dpae)(C ₂ (C ₆ H ₄)-4-OCH ₃)]	179
Table 4.34	Crystal data and structure refinement for [HRu ₃ (CO) ₇ (dpam)(C ₂ (C(CH ₃) ₃)]	183
Table 4.35	Selected Bond Lengths and Angles for[HRu ₃ (CO) ₇ (dpam)(C ₂ (C(CH ₃) ₃)]	185
Table 4.36	Crystal data and structure refinement for [HRu ₃ (CO) ₇ (dpam)(C ₂ (C ₆ H ₄)-4-OCH ₃)]	189
Table 4.37	Selected Bond Lengths and Angles for [HRu ₃ (CO) ₇ (dpam)(C ₂ (C ₆ H ₄)-4-OCH ₃)]	191
Table 4.38	Crystal data and structure refinement for [Ru ₃ (dpam)(COC ₆ H ₅)(CO) ₉]	194
Table 4.39	Selected Bond Lengths and Angles for [Ru ₃ (dpam)(COC ₆ H ₅)(CO) ₉]	196
Table 4.40	Spectroscopy data for Ru ₃ clusters with alkyne ligands	197
Table 4.41	Crystal data and structure refinement for Sb(C ₆ H ₄ -3-OCH ₃) ₃	201
Table 4.42	Selected Bond Lengths and Angles for Sb(C ₆ H ₄ -3-OCH ₃) ₃	203
Table 4.43	Crystal data and structure refinement for [Sb((C ₆ H ₄)SCH ₃) ₃]Cl ₂	206

Table 4.44	Selected Bond Lengths and Angles for [Sb((C ₆ H ₄)SCH ₃) ₃]Cl ₂	208
Table 4.45	Antiproliferative effect of [Sb((C ₆ H ₄)SCH ₃) ₃]Cl ₂ on different Human cancer cell lines	209
Table 4.46	Crystal data and structure refinement for [Ru ₃ (CO) ₁₀ (COC ₆ H ₄ OCH ₃)(Sb(C ₆ H ₄ -3-OCH ₃) ₂)]	216
Table 4.47	Selected Bond Lengths and Angles for [Ru ₃ (CO) ₁₀ (COC ₆ H ₄ OCH ₃)(Sb(C ₆ H ₄ -3-OCH ₃) ₂)]	218
Table 4.48	Crystal data and structure refinement for [Ru ₃ (CO) ₉ (dppm)(Sb(C ₆ H ₄ -3-OCH ₃) ₃)]	222
Table 4.49	Selected Bond Lengths and Angles for [Ru ₃ (CO) ₉ (dppm)(Sb(C ₆ H ₄ -3-OCH ₃) ₃)]	224
Table 4.50	Crystal data and structure refinement for [Ru ₃ (CO) ₉ (dpae)(Sb(C ₆ H ₄ -3-OCH ₃) ₃)]	228
Table 4.51	Selected Bond Lengths and Angles for [Ru ₃ (CO) ₉ (dpae)(Sb(C ₆ H ₄ -3-OCH ₃) ₃)]	230
Table 4.52	Crystal data and structure refinement for [Ru ₃ (CO) ₁₀ (COC ₁₂ H ₉)(Sb(C ₁₂ H ₉) ₂)]	234
Table 4.53	Selected Bond Lengths and Angles for [Ru ₃ (CO) ₁₀ (COC ₁₂ H ₉)(Sb(C ₁₂ H ₉) ₂)]	236
Table 4.54	Crystal data and structure refinement for [Ru ₃ (CO) ₉ (dppm)(Sb(C ₁₂ H ₉)]	240
Table 4.55	Selected Bond Lengths and Angles for [Ru ₃ (CO) ₉ (dppm)(Sb(C ₁₂ H ₉) ₃)]	242
Table 4.56	Spectroscopy data for Ru ₃ clusters with antimony ligands	243

LIST OF FIGURES

		Page
Figure 1.1	a) $\text{Ph}_2\text{P}(\text{C}_6\text{H}_4)\text{SCH}_3$ and b) $\text{Ph}_2\text{PCH}_2\text{SPh}$.	8
Figure 1.2	b) $\text{CH}_3\text{-4-C}_6\text{H}_5\text{C}_2\text{H}$, b) $\text{CH}_3\text{O-4-C}_6\text{H}_5\text{C}_2\text{H}$, c) $(\text{CH}_3)_3\text{SiC}_2\text{H}$, and d) $\text{HC}_2\text{C}(\text{CH}_3)_3$	9
Figure 1.3	a) $\text{Sb}(\text{C}_6\text{H}_4\text{-3-OCH}_3)_3$ and b) $\text{Sb}(\text{C}_{12}\text{H}_9)_3$	10
Figure 2.1	a) $[\text{HRu}_3(\text{CO})_7(\text{dppm})\text{SC}(\text{CH}_3)_3]$, b) $[\text{HRu}_3(\text{Ph}_2\text{PC}_4\text{H}_2\text{S})(\text{CO})_9]$, c) $[\text{HRu}_3(\text{Ph}_2\text{PC}_4\text{H}_2\text{S})(\text{CO})_8(\text{Ph}_2\text{PC}_4\text{H}_3\text{S})]$, and d) $[\text{HRu}_3(\mu\text{-SC}_6\text{H}_4\text{PPh}_2)(\text{CO})_9]$	23
Figure 2.2	a) $[\text{Os}_3(\text{CO})_{10}\text{Ph}_2\text{P}(\text{C}_4\text{H}_3\text{S})_2]$, b) $[\text{HOs}_3(\text{CO})_9\{\text{Ph}_2\text{P}(\text{C}_4\text{H}_2\text{S})\}]$, c) $[\text{Os}_3(\text{CO})_9\text{Ph}_2\text{P}(\text{C}_4\text{H}_3\text{S})]$, and d) $[\text{HOs}_3(\text{CO})_8(\text{Ph}_2\text{P}(\text{C}_4\text{H}_2\text{S}))(\text{Ph}_2\text{P}(\text{C}_4\text{H}_3\text{S}))]$	26
Figure 2.3	a) $[\text{HRu}_3(\mu_3\text{-S})\{\mu_2\text{-S}(\text{SPPH}_2)(\text{PPH}_2)\text{N}\}(\text{CO})_8]$, b) $[\text{HRu}_3\{\text{S}(\text{SPPH}_2)(\text{PPH}_2)\text{N}\}(\text{CO})_9]$, c) $[\text{Os}_3(\text{CO})_{11}(\text{Ph}_2\text{PCH}_2\text{CH}_2\text{SMe})]$, and d) $1,2[\text{Os}_3(\text{CO})_{10}(\text{Ph}_2\text{PCH}_2\text{CH}_2\text{SMe})]$	27
Figure 2.4	$1,1[\text{Os}_3(\text{CO})_{10}(\text{Ph}_2\text{PCH}_2\text{CH}_2\text{SMe})]$	28
Figure 2.5	a) $[\text{HRu}_3(\text{dppm})(\text{CO})_7(\text{SCH}_2\text{CH}_2\text{PPh})]$, b) $[\text{HRu}_3(\text{dppm})(\text{CO})_8(\text{SCH}_2\text{CH}_2\text{PPh})]$ $\text{Ru}_3(\text{dppm})(\text{CO})_9]$, c) $[\text{Os}_3(\text{CO})_{11}(\text{PSSP})]_2$, and d) $1,2\text{-}[\text{Os}_3(\text{CO})_{10}(\text{PSSP})]$	30
Figure 2.6	a) $[\{\text{Os}_3(\text{CO})_{10}\}_2(\text{PSSP})]_2$ and b) $[\text{Ru}_3(\text{CO})_9(\text{dpam})(\text{Ph}_2\text{PCH}_2\text{SPh})]$	31
Figure 2.7	a) $[\text{HRu}_3(\text{CO})_9(\text{C}_2\text{C}(\text{CH}_3)_3)]$, b) $[\text{HRu}_3(\text{dppm})(\text{CO})_7(\text{C}_2\text{C}(\text{CH}_3)_3)]$, c) $[\text{HRu}_3(\text{CO})_9(\text{C}_2\text{C}=\text{CH}_2(\text{C}_6\text{H}_5))]$, and d) $[\text{HRu}_3(\text{dppm})(\text{CO})_7(\text{C}_2\text{CCH}_3(\text{OH})(\text{C}_6\text{H}_5))]$	34

Figure 2.8	a) $[\text{HRu}_3(\text{dppm})(\text{CO})_7(\text{CH}_2=\text{C}(\text{C}_6\text{H}_5)\text{C}_2)]$, b) $(\text{HRu}_3(\text{CO})_9(\text{C}_2(\text{C}_6\text{H}_5)))$, c) $[\text{HRu}_3(\text{dppm})(\text{CO})_7(\text{C}_2(\text{C}_6\text{H}_5))]$, and d) $[\text{HRu}_3(\text{dppm})(\text{CO})_9(\text{C}_2(\text{C}_6\text{F}_5))]$	35
Figure 2.9	a) $[\text{HRu}_3(\text{CO})_7(\text{dppm})(\text{C}_2\text{-c-C}_5\text{H}_7)]$ and b) $[\text{HRu}_3(\text{CO})_7(\text{dppm})(\text{C}_2\text{-c-C}_5\text{H}_6)]$	37
Figure 2.10	a) $[\text{HRu}_3(\text{CO})_9(\text{C}_2(\text{CH}_3\text{-4-C}_6\text{H}_5))]$, b) $[\text{HRu}_3(\text{CO})_9(\text{C}_2(\text{C}_6\text{H}_4\text{-4-NH}_2))]$, c) $[\text{HRu}_3(\text{CO})_9(\text{C}_2\text{CH}_2(\text{OH}))]$ and d) $[\text{HRu}_3(\text{CO})_9(\text{C}_2\text{C}\equiv\text{C}(\text{W}(\text{CO})_3\text{Cp}))]$	38
Figure 2.11	a) $[\text{HRu}_3(\text{CO})_7(\text{dppm})(\text{C}_2\text{C}_2(\text{W}(\text{CO})_3\text{Cp}))]$, b) $[\text{HRu}_3(\text{CO})_9(\text{C}_2(\eta^5\text{-C}_5\text{H}_5)(\text{Fe}(\text{CO})_2))]$, and c) $[\text{HRu}_3(\text{dppm})(\text{CO})_7(\text{C}_2\text{C}\equiv\text{CFc})]$	39
Figure 2.12	a) $[\text{HRu}_3(\text{CO})_9[\text{C}_2\text{Si}(\text{CH}_3)_3]]$, b) $[\text{HRu}_3(\text{CO})_9(\text{C}_2\text{Si}(\text{C}_6\text{H}_5)_3)]$, c) $[\text{HRu}_3(\text{CO})_9(\text{C}_2\text{Si}(\text{C}(\text{CH}_3)_2)_3)]$, and d) $[\text{HRu}_3(\text{CO})_7(\text{dppm})(\text{C}_2(\text{C}_6\text{H}_4)\text{C}\equiv\text{C}(\text{C}_6\text{H}_4\text{-4-CH}_3))]$	42
Figure 2.13	a) $[\text{HRu}_3(\text{CO})_9(\text{C}_2\text{C}_6\text{H}_4\text{-4-C}(\text{CH}_3)_3)]$, b) $[\text{HRu}_3(\text{CO})_9(\text{C}_2(\text{C}_6\text{H}_3)\text{-2,5-}(\text{CH}_3)_2)]$, c) $[\text{HRu}_3(\text{CO})_9(\text{C}_2(\text{C}_6\text{H}_2)\text{-2,4,5-}(\text{CH}_3)_3)]$, and d) $[\text{HRu}_3(\text{CO})_7(\text{dppe})(\text{C}_2\text{C}_6\text{H}_3\text{-2,5-}(\text{CH}_3)_2)]$	43
Figure 2.14	a) $[\text{HRu}_3(\text{CO})_7(\text{dppm})(\text{C}_2\text{-4-bpy})]$ and b) $[\text{HRu}_3(\text{CO})_7(\text{dppm})(\text{C}_2\text{-5-bpy})]$	44
Figure 2.15	a) $[\text{Ru}_3(\text{COC}_6\text{H}_5)(\text{CO})_{10}(\text{Sb}(\text{C}_6\text{H}_5)_2)]$, b) $[\text{Ru}_3(\text{CO})_9(\text{dppm})(\text{SbPh}_3)]$, c) $[\text{Ru}_3(\text{CO})_{10}(\text{dpam})(\text{SbPh}_3)]$, and d) $[\text{Ru}_3(\text{CO})_{10}(\text{dppe})(\text{SbPh}_3)]$	46
Figure 2.16	$[\text{H}_3\text{Ru}_6(\mu_5\text{-Sb})(\text{CO})_{18}(\text{SbPh}_3)]$	47
Figure 2.17	a) $[\text{Ru}_3(\text{CO})_{10}(\mu\text{-H})(\mu\text{-SbPh}_2)]$, b) $[\text{Ru}_3(\text{CO})_{10}(\mu\text{-SbPh}_2)(\text{SbPh}_2)]$, c) $[\text{Ru}_3(\text{CO})_9(\mu\text{-SbPh}_2)(\text{SbPh}_2\text{PPh}_3)]$, and d) $[\text{Ru}_3(\text{CO})_9(\mu\text{-SbPh}_2)(\text{SbPh}_2)(\text{AsPh}_3)]$	49
Figure 2.18	a) $[\text{Ru}_3(\text{CO})_9(\mu\text{-SbPh}_2)(\text{SbPh}_2\text{SbPh}_3)]$ b) $[\text{Ru}_3(\text{CO})_9(\mu\text{-SbPh}_2)(\mu\text{-SbPh}_2)_2(\text{Cl})]$ c) $\text{Ru}_3(\text{CO})_8(\mu\text{-SbPh}_2)(\mu\text{-SbPh}_2)_2(\text{Cl})(\text{SbPh}_2\text{CH}_2\text{Cl})$	50

Figure 4.1	The ORTEP diagram of $\text{Ph}_2\text{PC}_6\text{H}_4\text{SCH}_3$	83
Figure 4.2	The ORTEP diagram of $\text{Ph}_2\text{PCH}_2\text{SPh}$	84
Figure 4.3	The ORTEP diagram of $[\text{Ru}_3(\text{CO})_{11}(\text{PPh}_2\text{C}_6\text{H}_4\text{SCH}_3)]$	92
Figure 4.4	The ORTEP diagram of $[\text{Ru}_3(\text{CO})_9(\text{dppe})(\text{PPh}_2\text{C}_6\text{H}_4\text{SCH}_3)]$	98
Figure 4.5	The ORTEP diagram of $[\text{Ru}_3(\text{CO})_9(\text{dppm})(\text{PPh}_2\text{C}_6\text{H}_4\text{SCH}_3)]$	104
Figure 4.6	The ORTEP diagram of $[\text{Ru}_3(\text{CO})_9(\text{dpam})(\text{PPh}_2\text{C}_6\text{H}_4\text{SCH}_3)]$	110
Figure 4.7	The ORTEP diagram of $[\text{Ru}_3(\text{CO})_9(\text{dotpm})(\text{Ph}_2\text{PCH}_2\text{SPh})]$	116
Figure 4.8	The ORTEP diagram of $[\text{Os}_3(\text{CO})_{11}(\text{PPh}_2\text{C}_6\text{H}_4\text{SCH}_3)]$	122
Figure 4.9	The ORTEP diagram of $[\text{Os}_3(\text{CO})_{11}(\text{Ph}_2\text{PCH}_2\text{SPh})]$	128
Figure 4.10	The ORTEP diagram of $[\text{Os}_3(\text{CO})_{10}(\mu\text{-Ph}_2\text{PCH}_2\text{SPh})]$	134
Figure 4.11	The ORTEP diagram of $[\text{HRu}_3(\text{CO})_7(\text{dppm})(\text{C}_2(\text{C}_6\text{H}_4)\text{-4-OCH}_3)]$	142
Figure 4.12	The ORTEP diagram of $[\text{HRu}_3(\text{CO})_7(\text{dppe})(\text{C}_2\text{Si}(\text{CH}_3)_3)]$	148
Figure 4.13	The ORTEP diagram of $[\text{HRu}_3(\text{CO})_7(\text{dppe})(\text{C}_2(\text{C}_6\text{H}_4)\text{-4-OCH}_3)]$	154
Figure 4.14	The ORTEP diagram of $[\text{HRu}_3(\text{CO})_7(\text{dppf})(\text{C}_2\text{Si}(\text{CH}_3)_3)]$	160
Figure 4.15	The ORTEP diagram of $[\text{HRu}_3(\text{CO})_7(\text{dppf})(\text{C}_2(\text{C}_6\text{H}_4)\text{-4-OCH}_3)]$	166
Figure 4.16	The ORTEP diagram of $[\text{HRu}_3(\text{CO})_7(\text{dpae})(\text{C}_2\text{Si}(\text{CH}_3)_3)]$	172
Figure 4.17	The ORTEP diagram of $[\text{HRu}_3(\text{CO})_7(\text{dpae})(\text{C}_2(\text{C}_6\text{H}_4)\text{-4-OCH}_3)]$	178

Figure 4.18	The ORTEP diagram of [HRu ₃ (CO) ₇ (dpam)(C ₂ C(CH ₃) ₃)]	184
Figure 4.19	The ORTEP diagram of [HRu ₃ (CO) ₇ (dpam)(C ₂ (C ₆ H ₄ -4-CH ₃))]	190
Figure 4.20	The ORTEP diagram of [Ru ₃ (CO) ₉ (dpam)(COC ₆ H ₅)]	195
Figure 4.21	The ORTEP diagram of Sb(C ₆ H ₄ -3-OCH ₃) ₃	202
Figure 4.22	The ORTEP diagram of [Sb((C ₆ H ₄)SCH ₃) ₃]Cl ₂	207
Figure 4.23	Dose-dependent anti-proliferative effect of Sb{(C ₆ H ₄)SCH ₃ } ₃ Cl ₂	211
Figure 4.24	Photomicrographic images of cancer cell lines, 48 hours after treatment with the Sb{(C ₆ H ₄)SCH ₃ } ₃ Cl ₂	212
Figure 4.25	The ORTEP diagram of [Ru ₃ (CO) ₁₀ (COC ₆ H ₄ OCH ₃) (Sb(C ₆ H ₄ -3-OCH ₃) ₂)]	217
Figure 4.26	The ORTEP diagram of [Ru ₃ (CO) ₉ (dppm)(Sb(C ₆ H ₄ - 3-OCH ₃) ₃)]	223
Figure 4.27	The ORTEP diagram of [Ru ₃ (CO) ₉ (dpae)(Sb(C ₆ H ₄ -3- OCH ₃) ₃)]	229
Figure 4.28	The ORTEP diagram of [Ru ₃ (CO) ₁₀ (COC ₁₂ H ₉)(Sb(C ₁₂ H ₉) ₂)]	235
Figure 4.29	The ORTEP diagram of [Ru ₃ (CO) ₉ (dppm)(Sb(C ₁₂ H ₉) ₃)]	241

LIST OF SCHEMES

		Page
Scheme 2.1	Catalytic cycle of benzophenone ketyl radical anion reaction mechanism	14

LIST OF ABBREVIATIONS

Å	angstrom
a, b, c	unit cell dimensions
anal	analysis atoms standard
ax	axial
ax	exial
BPK	sodium benzophenone ketyl radical anion $\text{Na}^+[\text{PhCOPh}]^{\cdot -}$
bpy	bipyridine
(bpcd)	4,5-bis(diphenyl-phosphino)-4-cyclopenten-1,3-dione
Bu ^t	tertbutyl -C(CH ₃) ₃
Calc	calculated

°C	degree Centigrade
cm	centimetre (10^{-2} m)
cm ³	cubic centimetre
Cp	cyclopentadienyl
dcpm	Bis(dicyclohexylphosphino)methane
dpae	1,2-bis(diphenylarsino)ethane
dpam	bis(diphenylarsino)methane
dppa	bis(diphenylphosphino)acetylene
dppe	1,2-bis(diphenylphosphino)ethane
dppf	1,1'-bis(diphenylphosphino)ferrocene $\text{Fe}(\text{C}_5\text{H}_4\text{PPh}_2)_2$
dppm	bis(diphenylphosphino)methane
e	electron
eq	equatorial

et	ethyl
ffars	1,2-bis(dimethylarsino)butaflouro-cyclobutene
ffos	1,2-bis(diphenylphosphino)butaflouro-cyclobutene
f ₆ fos	1,2-bis(diphenylphosphino)hexaflouro-cyclohexene
g	gram
h	hour
Hz	hertz
IR	infrared
J	coupling constant
L	general monodentate ligand
L-L	general bidentate ligand

m.p	melting point
mapm	diphenyl(o-N,N-dimethylaniliny) phosphine
Me	methyl
mg	milligram
MHz	megahertz
min	minutes
ml	milliliter
mmol	millimole
mol	mole
OD _b	Optical density of the blank
OD _n	Optical density of the negative control
OD _s	Optical density of the samples

ORTEP	Oak Ridge Thermal Ellipsoid Plot
Ph	phenyl
ppm	part per million
PPN ⁺	bis(triphenylphosphino) iminium (Ph ₃ P) ₂ N ⁺
Pr ⁱ	iso-propyl
R	alkyl
R _f	retention factor
SADABS	Siemens Area Detector Absorption Correction
SAINT	Siemens Analytical X-ray Area-detector Integration
sec	seconds
THF	tetrahydrofuran
TLC	thin layer chromatography

TMS	tetramethylsilane
α, β, γ	unit cell angles
μ	bridging bonding mode
NMR	nuclear magnetic resonance
^{13}C	carbon-13 isotope
d	doublet
dd	doublet of doublet
dt	doublet of the triplet
^1H	proton
m	multiplet
q	quartet
s	singlet

t triplet

td triplet of the doublet

**SINTESIS DAN PENCIRIAN GUGUSAN Ru₃ DAN Os₃ DENGAN
SULFUR YANG MENGANDUNGI LIGAN PHOSPHINA, ACETILENA,
DAN ANTIMONI**

ABSTRAK

Dua puluh empat kompleks gugusan baharu; dua puluh satu kompleks gugusan triruthenium carbonil, tiga kompleks gugusan triosmium carbonil dan empat ligan telah berjaya disintesis dan dicirikan menggunakan kaedah analisis unsur, dan kaedah spektroskopi, merangkumi IR, ¹H NMR, ¹³C NMR dan ³¹P NMR spektroskopi. Struktur molekul produk telah ditentukan oleh kristal tunggal pembelauan sinar-X kecuali Ru₃(CO)₁₀(dpae). Dua ligan isomer daripada C₁₉H₁₇PS; iaitu PPh₂C₆H₄SMe dan Ph₂PCH₂SPh. Dua ligan antimoni Sb(C₆H₄-3-OCH₃)₃ dan Sb(C₁₂H₉)₃ digunakan bagi membentuk gugusan baharu. Satu sebatian antimony [Sb((C₆H₄)SCH₃)₃Cl₂] diuji bagi potensi anti-kanser terhadap beberapa jalur sel kanser manusia, iaitu kolon kanser (HCT- 116 and HT-29), kanser payudara (MCF-7), dan leukemia (K-562), sel kolon normal manusia (CCD-18Co) digunakan sebagai kawalan bagi model jalur sel normal. Keputusan menunjukkan sebatian yang diuji mempamerkan kesan anti-proliferatif terhadap semua jalur sel kanser. Keputusan ujian sitotoksiti boleh menjadi panduan kepada penemuan ubat. Tindak balas Ru₃(CO)₁₂ dan Os₃(CO)₁₂ dengan kedua-dua ligan sulfur fosforus menghasilkan tiga gugusan monotertukarganti;

$\text{Ru}_3(\text{CO})_{11}\text{PPh}_2\text{C}_6\text{H}_4\text{SCH}_3$, $\text{Os}_3(\text{CO})_{11}\text{PPh}_2\text{C}_6\text{H}_4\text{SCH}_3$, $\text{Os}_3(\text{CO})_{11}\text{Ph}_2\text{PCH}_2\text{SPh}$,
 dan gugusan dwitertukarganti $\text{Os}_3(\text{CO})_{10}\text{Ph}_2\text{PCH}_2\text{SPh}$. Tambahan pula, empat
 kelompok tritertukarganti dihasilkan iaitu $\text{Ru}_3(\text{CO})_9(\text{dppe})\text{PPh}_2\text{C}_6\text{H}_4\text{SCH}_3$,
 $\text{Ru}_3(\text{CO})_9(\text{dppm})\text{PPh}_2\text{C}_6\text{H}_4\text{SCH}_3$, $\text{Ru}_3(\text{CO})_9(\text{dpam})\text{PPh}_2\text{C}_6\text{H}_4\text{SCH}_3$ dan $\text{Ru}_3(\text{CO})_9$
 $(\text{dotpm})\text{Ph}_2\text{PCH}_2\text{SPh}$ dari reaksi $\text{Ru}_3(\text{CO})_{10}(\text{LL})$ dengan dua P, S ligan. Ligan
 monodentat dan ligan bidentat menduduki kedudukan khatulistiwa atas sebab
 sterik. Ikatan Ru-Ru yang paling panjang adalah *cis* kepada ligan P, S
 monodentat melainkan bagi gugusan $\text{Os}_3(\text{CO})_{10}\text{Ph}_2\text{PCH}_2\text{SPh}$ ikatan Ru-Ru yang
 paling panjang adalah ikatan di antara ligan bidentat P, S. Untuk semua gugusan,
 ikatan Ru-C pada kedudukan paksi lebih panjang daripada CO pada kedudukan
 khatulistiwa. Tindak balas $\text{Ru}_3(\text{CO})_{10}(\text{LL})$, dengan empat asetilena hujung yang
 berbeza iaitu $\text{HC}_2\text{Si}(\text{CH}_3)_3$, $\text{HC}_2(\text{C}_6\text{H}_4)\text{-4-OCH}_3$, $\text{HC}_2\text{C}(\text{CH}_3)_3$, dan $\text{HC}_2(\text{C}_6\text{H}_4)\text{-4-}$
 CH_3 menghasilkan $[\text{HRu}_3(\text{CO})_7(\text{dppe})(\text{C}_2\text{Si}(\text{CH}_3)_3)]$, $[\text{HRu}_3(\text{CO})_7(\text{dppf})$
 $(\text{C}_2\text{Si}(\text{CH}_3)_3)]$, $[\text{HRu}_3(\text{CO})_7(\text{dpae})(\text{C}_2\text{Si}(\text{CH}_3)_3)]$, $[\text{HRu}_3(\text{CO})_7(\text{dppm})(\text{C}_2(\text{C}_6\text{H}_4)\text{-}$
 $4\text{-OCH}_3)]$, $[\text{HRu}_3(\text{CO})_7(\text{dppe})(\text{C}_2(\text{C}_6\text{H}_4)\text{-4-OCH}_3)]$, $[\text{HRu}_3(\text{CO})_7(\text{dppf})$
 $(\text{C}_2(\text{C}_6\text{H}_4)\text{-4-OCH}_3)]$, dan $[\text{HRu}_3(\text{CO})_7(\text{dpae})(\text{C}_2(\text{C}_6\text{H}_4)\text{-4-OCH}_3)]$, $[\text{HRu}_3(\text{CO})_7$
 $(\text{dpam})(\text{C}_2\text{C}(\text{CH}_3)_3)]$, $[\text{HRu}_3(\text{CO})_7(\text{dpam})(\text{C}_2(\text{C}_6\text{H}_4)\text{-4-CH}_3)]$. Suatu struktur yang
 unik triruthenium terbuka $[\text{Ru}_3(\text{CO})_9(\text{dpam})(\text{COC}_6\text{H}_5)]$, adalah (COC_6H_5) asil
 berhubung kepada Ru1---Ru3. Selain itu, atom arsenik kedua, AS(2) juga
 berhubung kepada Ru1---Ru3. Tindak balas $\text{Ru}_3(\text{CO})_{12}$ dengan kedua-dua ligan
 antimoni; $\text{Sb}(\text{C}_6\text{H}_4\text{-3-OCH}_3)_3$ dan $\text{Sb}(\text{C}_{12}\text{H}_9)_3$ menghasilkan dua kelompok
 triruthenium terbuka $\text{Ru}_3(\text{CO})_{10}(\text{COC}_6\text{H}_4\text{-3-OCH}_3)\text{Sb}(\text{C}_6\text{H}_4\text{-3-OCH}_3)_2$ dan
 $[\text{Ru}_3(\text{CO})_{10}(\text{COC}_{12}\text{H}_9)(\text{Sb}(\text{C}_{12}\text{H}_9)_2)]$. $(\text{COC}_6\text{H}_4\text{-3-OCH}_3)$ dan $(\text{CO C}_{12}\text{H}_9)$ asil

berhubung kepada Ru1---Ru3. Tambahan pula, tindak balas $\text{Ru}_3(\text{CO})_{10}(\text{dppm})$, $\text{Ru}_3(\text{CO})_{10}(\text{dpae})$ dengan dua ligan antimoni; menghasilkan tiga kelompok tritertukarganti $[\text{Ru}_3(\text{CO})_9(\text{dppm})(\text{Sb}(\text{C}_6\text{H}_4\text{-3-OCH}_3)_3)]$, $[\text{Ru}_3(\text{CO})_9(\text{dpae})(\text{Sb}(\text{C}_6\text{H}_4\text{-3-OCH}_3)_3)]$, dan $[\text{Ru}_3(\text{CO})_9(\text{dppm})(\text{Sb}(\text{C}_{12}\text{H}_9)_3)]$. Ikatan Ru-Ru paling panjang adalah *cis* kepada ligan antimoni monodentat. Bagi semua kelompok, ikatan Ru-C lebih panjang pada kedudukan CO paksi daripada CO khatulistiwa.

**SYNTHESIS AND CHARACTERISATION OF NEW Ru₃ AND Os₃
CLUSTERS WITH SULPHUR CONTAINING PHOSPHINES, ALKYNE,
AND ANTIMONY LIGANDS**

ABSTRACT

Twenty four new clusters; twenty one new triruthenium carbonyl clusters, three triosmium carbonyl clusters, and four new ligands were successfully synthesised and characterised by elemental analysis and spectroscopic methods, including IR, ¹H NMR, ¹³C NMR and ³¹P NMR spectroscopy. Molecular structures of the crystallised products were determined by single crystal X-ray diffraction except for Ru₃(CO)₁₀(dpae). Two isomer ligands of C₁₉H₁₇PS; namely PPh₂C₆H₄SMe and Ph₂PCH₂SPh, two antimony ligands Sb(C₆H₄-3-OCH₃)₃ and Sb(C₁₂H₉)₃ were used to form clusters. One antimony compound [Sb((C₆H₄)SCH₃)₃Cl₂], was tested for its anticancer potential against several human cancerous cell lines, namely colon (HCT- 116 and HT-29), breast (MCF-7) and Leukemia (K-562) cell lines. Human normal colon cells (CCD-18Co) as control were used as a model cell line for normal cells. The result revealed that the tested compound showed promising antiproliferative effects on all cancer cell lines. The result of cytotoxicity test could be a good lead for drug discovery. The reaction of Ru₃(CO)₁₂ and Os₃(CO)₁₂ with the sulphur containing phosphines bidentate ligands produced three monosubstituted clusters; [Ru₃(CO)₁₁(PPh₂C₆H₄SCH₃)], [Os₃(CO)₁₁

(PPh₂C₆H₄SCH₃), [Os₃(CO)₁₁(Ph₂PCH₂SPh)], and one disubstituted cluster, [Os₃(CO)₁₀(Ph₂PCH₂SPh)]. Furthermore, four trisubstituted clusters [Ru₃(CO)₉(dppe)(PPh₂C₆H₄SCH₃)], [Ru₃(CO)₉(dppm)(PPh₂C₆H₄SCH₃)], [Ru₃(CO)₉(dpam)(PPh₂C₆H₄SCH₃)], and [Ru₃(CO)₉(dotpm)(Ph₂PCH₂SPh)] were obtained from the reaction of [Ru₃(CO)₁₀(LL)] with the sulphur containing phosphines bidentate ligands. Monodentate and bidentate ligands occupy the equatorial position for a steric reason. The longest Ru-Ru bond is *cis* to the sulphur containing phosphines ligands. Except for [Os₃(CO)₁₀(Ph₂PCH₂SPh)], the longest Ru-Ru bond is the bond between the bidentate sulphur containing phosphines ligands. For all the clusters, the Ru-C bonds are longer for axial CO than equatorial CO. The reaction of [Ru₃(CO)₁₀(LL)], with four different terminal acetylenes namely HC₂Si(CH₃)₃, HC₂(C₆H₄)-4-OCH₃, HC₂C(CH₃)₃, and HC₂(C₆H₄)-4-CH₃ produced [HRu₃(CO)₇(dppe)(C₂Si(CH₃)₃)], [HRu₃(CO)₇(dppf)(C₂Si(CH₃)₃)], [HRu₃(CO)₇(dpae)(C₂Si(CH₃)₃)], [HRu₃(CO)₇(dppm)(C₂(C₆H₄)-4-OCH₃)], [HRu₃(CO)₇(dppe)(C₂(C₆H₄)-4-OCH₃)], [HRu₃(CO)₇(dppf)(C₂(C₆H₄)-4-OCH₃)], [HRu₃(CO)₇(dpae)(C₂(C₆H₄)-4-OCH₃)], [HRu₃(CO)₇(dpam)(C₂C(CH₃)₃)], and [HRu₃(CO)₇(dpam)(C₂(C₆H₄)-4-CH₃)]. A novel compound of open triruthenium [Ru₃(CO)₉(dpam)(COC₆H₅)], the (COC₆H₅) acyl is bridging Ru(1)---Ru(3) atoms. The second arsenic atom, As(2) is also bridging Ru(1)---Ru(3) atoms. The reaction of Ru₃(CO)₁₂ with the two antimony ligands, Sb(C₆H₄-3-OCH₃)₃ and Sb(C₁₂H₉)₃ produced two open triruthenium clusters [Ru₃(CO)₁₀(COC₆H₄-3-OCH₃)(Sb(C₆H₄-3-OCH₃)₂)] and [Ru₃(CO)₁₀(COC₁₂H₉)(Sb(C₁₂H₉)₂)]. The (COC₆H₄-3-OCH₃) and (COC₁₂H₉) acyl are bridging

Ru(1)---Ru(3) atoms. Furthermore, the reaction of $[\text{Ru}_3(\text{CO})_{10}(\text{dppm})]$, $[\text{Ru}_3(\text{CO})_{10}(\text{dpae})]$ with the two antimony ligands; produced three trisubstituted clusters $[\text{Ru}_3(\text{CO})_9(\text{dppm})(\text{Sb}(\text{C}_6\text{H}_4\text{-3-OCH}_3)_3)]$, $[\text{Ru}_3(\text{CO})_9(\text{dpae})(\text{Sb}(\text{C}_6\text{H}_4\text{-3-OCH}_3)_3)]$, and $[\text{Ru}_3(\text{CO})_9(\text{dppm})(\text{Sb}(\text{C}_{12}\text{H}_9)_3)]$. The longest Ru-Ru bond is *cis* to the monodentate antimony ligand. For all the clusters, the Ru-C bonds are longer for axial CO than equatorial CO.

CHAPTER 1

INTRODUCTION

1.1 Metal clusters chemistry

Intensive study of the chemistry of transition metal clusters started in the middle of the last century. Organometallic cluster chemistry lies as a link between pure organic and inorganic chemistry as it involves the influence of inorganic metal ions and organic molecules or organic functional groups. The metal cluster provides a framework in which ligands are capable of coordination with one or more metal centres [1].

Cluster molecules are formed from the coordination of π -acceptor ligands and transition metal atoms, in particular, ligands such as carbon monoxide, cyclopentadienyl, and phosphine. The π -acceptor ligands help to produce the most stable condition for the metal-metal bond formation of the Group 8 elements by inducing the high overlap between the atomic orbitals of the metal. The formation of metal-metal bonds is necessary to construct cluster complexes. The bonding between metal and carbon monoxide, always involves coordination of the carbon atom, through the donation of the 2e on the carbon atom to an empty metal d orbital of σ symmetry, and a back donation from filled metal d orbitals to the empty π^* C-O antibonding orbital.

A cluster defined as a molecule containing three or more metal atoms connected by direct metal-metal bonds. Triruthenium dodecacarbonyl $\text{Ru}_3(\text{CO})_{12}$ and triosmium dodecacarbonyl $\text{Os}_3(\text{CO})_{12}$, have three metal atoms linked by the metal - metal bond. Each Ru and Os atom carries four terminal carbonyl ligands. Two carbonyl ligands are equatorial because parallel to the plane of the Ru_3 and Os_3 triangle, the other two are axial because they are vertical to the Ru_3 and Os_3 triangle [2].

The type of ligands can also affect the nuclearity and geometry of the cluster by extending its steric effect. For example, as the ligand size increases, the rates of reactions leading to metal-metal bond formation are reduced and for a given ligand: metal ratio, the higher-nuclearity clusters are destabilised by ligand-ligand repulsion effects [3].

The properties of the metal cluster that are built from three or more metal centre help to facilitate activation and transformation of the substrates and high mobility of the ligands could promote reactions between several molecules bonded to the cluster framework [2]. The study of the metal clusters is interesting mostly because metal clusters can act as homogeneous catalysts [4,5]. The metal cluster has played a significant role in many chemical reactions, for example, they act as catalysts for carbonylation of alcohols [6,7], hydrogenation, isomerization of olefins [6–10], and water gas shift reaction and hydroformylation of alkenes [11].

These clusters of triruthenium and triosmium are of concern in the oil industry, especially those containing large amounts of sulphur compounds that require

hydrodesulphurisation (HDS) and hence are of interest environmentally and industrially [12–15]. Ruthenium compounds show anticancer activities and reduce the potential for tumour resistance and can be a significant chemotherapy for cancer cells [16–20].

1.1.1 Triiron Dodecacarbonyl

Triiron dodecacarbonyl was first synthesised in 1906 by the thermal decomposition of $\text{Fe}_2(\text{CO})_9$. In 1930 Hieber and Becker synthesised $\text{Fe}_3(\text{CO})_{12}$ from freezing point depression studies in iron pentacarbonyl solvent. In 1951 it was characterised as $\text{Fe}_3(\text{CO})_{12}$ by Sheline. In 1968, Wei and Dahl characterised and formulated $\text{Fe}_3(\text{CO})_{12}$ consisting of three identical $\text{Fe}(\text{CO})_3$ and linked in pairs to one another by a bridging carbonyl group and an iron-iron bond [21].

1.1.2 Triruthenium dodecacarbonyl

Triruthenium dodecacarbonyl was synthesised in 1910 by Mond and co-workers, from the reaction of ruthenium metal with carbon monoxide at 300 °C and 400 atmosphere pressure. The product obtained was a triruthenium carbonyl, but it was not correctly characterised [22]. Then, Corey and Dahl in 1961 characterised and formulated it as $\text{Ru}_3(\text{CO})_{12}$ by X-ray crystallography [23]. In 1966, Bruce and Stone published an improved synthesis of $\text{Ru}_3(\text{CO})_{12}$ by carbonylation of ruthenium trichloride in methanol at 65°C and less than 10 atmosphere pressure in the presence of halogen acceptors [24]. Later in 1983, Bruce and co-workers reported a new

preparation of $\text{Ru}_3(\text{CO})_{12}$ by the carbonylation of a 1% methanol solution of hydrated ruthenium trichloride at 50-60 atmosphere pressure and 125 °C for 16–18 h [25].

1.1.3 Triosmium dodecacarbonyl

Triosmium dodecacarbonyl was synthesised in 1943 by Hieber, as $\text{Os}_2(\text{CO})_9$. The reaction of OsO_4 with HI gave an oxy iodide, which was treated with Ag powder in benzene with carbon monoxide at 150 °C and (200 atm) to give $\text{Os}_3(\text{CO})_{12}$ in poor yield. Corey and Dahl in 1961 characterised and formulated it as $\text{Os}_3(\text{CO})_{12}$ by X-ray crystal structure [23]. Triosmium dodecacarbonyl has been one of the opener compounds in the evolution of transition-metal clusters, because it can produce a lot of new clusters, often without any change of nuclearity. Triosmium dodecacarbonyl reactive derivatives; $\text{Os}_3\text{H}_2(\text{CO})_{10}$ [10], $\text{Os}_3(\text{CO})_{11}\text{L}$, and $\text{Os}_3(\text{CO})_{10}\text{LL}$ are useful starting material for triosmium Clusters, and hundreds of compounds had been produced, where L and LL are labile ligands [26].

Many types of ligands have the potential to substitute with these transition metal carbonyl clusters, depending on the coordination reactivity of these ligands [2]. This contribute to an idea of substituting different ligands with a variety of chemical and physical properties to transition metal carbonyl clusters.

1.2 Ligands

Ligands are neutral molecules or ions that bond to a central metal atom or ion to form a complex. Ligands donate a pair of electrons or more (Lewis bases), and the central atom receives the pair of electrons or more (Lewis acid). Ligands are classified due to the number of donor atoms as monodentate, bidentate, and polydentate. They are also classified as cations, anions, or neutral molecules [27].

1.2.1 Bidentate ligands (L-L) Types (P- P) and (As-As)

Bidentate ligands are defined as ligands that can form two bonds with metals. An important Group 15 ligand is bidentate phosphine and arsine that contains a carbon backbone linking the Group 15 element. For example, the most common bidentate phosphine ligands are of the type $\text{PPh}_2(\text{CH}_2)_n\text{PPh}_2$, where $n= 1-6$ which have been widely used in organometallic reactions over the years [28–33]. Also, bidentate ligands can possess two different Group 15 donor atoms known as a mixed bidentate ligand. For example, the arphos ligand with chemical formula, $\text{Ph}_2\text{PCH}_2\text{CH}_2\text{AsPh}_2$, is a mixed bidentate ligand with As and P atoms linked by two methylene carbon backbone [31].

Bidentate ligands can play a role in stabilising metal cluster by coordinating in different modes. The bidentate ligand has been found to arrange a variety of bonding modes on the cluster, including monodentate, chelating a single metal atom in the cluster, bridging across a metal-metal bond, and forming an intermolecular link

across two triangle clusters. Reactions conducted by Bruce and co-workers in 1982 which deal with $\text{Ru}_3(\text{CO})_{12}$ and bis(diphenyl phosphino)ethane (dppe) were reported to function as a monodentate, bidentate and chelating ligand. Moreover, they served as a bridging ligand across a metal-metal bond, connecting a ligand in the cluster. $[\text{Ru}_3(\text{CO})_{11}]_2\text{dppe}$, $[\text{Ru}_3(\text{CO})_{11}]_2\text{dppb}$, and $[\text{Ru}_3(\text{CO})_{11}]_2\text{dppf}$, whereby two metal cluster units bonded through di-tertiary phosphine ligands [28,34,35]. Particularly, diphosphines such as dppm, dppe, dppf, dcpm, and dpam are in widespread use in homogeneous catalysis [31,36].

The design, synthesis, and characterization of metal cluster complexes are essential in providing a suitable array of the cluster that contains the necessary stoichiometry and binding required for understanding the electronic influence as well as the effect of the different ligands on the chemical behaviour of their cluster complexes. Nevertheless, metal clusters showed a significant role in the industry as homogeneous catalysts [5,37]. Moreover, as precursors to bi- and trimetallic nanoparticle catalysts in heterogeneous catalysis[38], detailed knowledge of the bonding and geometry structure of these clusters are needed in providing a route from fundamental to applied science in this area of study. Research about the synthesis, characterization and molecular structure which are resulted from the substitution of CO with diphosphine and diarsine ligands are necessary to understand the electronic and steric effects of the new cluster.

1.2.2 Sulphur containing phosphines ligands

In fact, a ligand containing one strongly binding donor atom and one weakly binding donor atom are used to maintain an active site at a metal centre until it is required to effect a transformation of a substrate. Ligands containing phosphorus centres and sulphur centres are significant. Both phosphorus and sulphur are common ligand donor atoms for a broad range of metals while the existence of several lone pairs of electrons and the low ionisation energy of sulphur offers the possibility of a rich sulfur-based chemistry of the complexes [37].

The (P, S) ligands with $\text{Ru}_3(\text{CO})_{12}$ and $\text{Os}_3(\text{CO})_{12}$ react as monodentate, through phosphorus [13,15,39,40], and as bidentate ligands bridging or chelating through phosphorus and sulphur [12–14,41–43]. Phosphorus atom in (P, S) ligands donates 2 electrons when bonded to one metal atom, 3 electrons when bridging two metal atoms, and has the priority to connect with triruthenium and triosmium. Phosphorus ligands are strong σ -donors and poor π -acceptors [2]. Sulfur in (P, S) ligands can donate; 2 electrons, when bonded to one metal atom [42,43], 3 electrons (μ_2) when bridging two metal atoms [12,14,41], 4 electrons (μ_3) [41] and 5 electrons (μ_3) when capping three metal atoms [44].

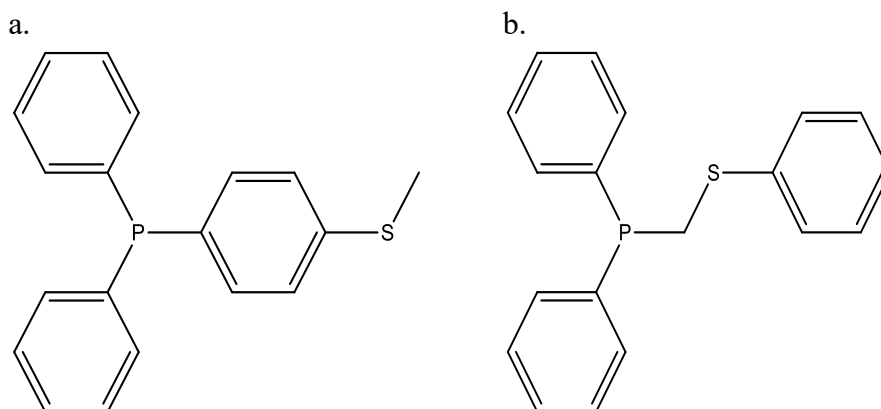


Figure 1.1 a) $\text{Ph}_2\text{P}(\text{C}_6\text{H}_4)\text{SCH}_3$ and b) $\text{Ph}_2\text{PCH}_2\text{SPh}$.

1.2.3 Alkyne ligands

The reactions of terminal alkynes with trinuclear ruthenium clusters lead to hydrogen transfer to the metals centre [45]. The alkyne ligands react with triruthenium dodecacarbonyl to give clusters containing $\mu\text{-H}$ and $\mu\text{-alkynyl}$ group. Alkynyl group donate 5 electrons through two types of bonds, Ru-C σ -bond, donate 1 electron and the $\text{C}\equiv\text{C}$ bond bridging the other two Ru atoms by π bonds, donate 4 electrons. The $\mu\text{-H}$ located between the same two Ru atoms which are connected to $\text{C}\equiv\text{C}$ bond by π bonds. The $\text{HC}\equiv\text{CR}$ is then considered as a 6 electrons donor ligand [46]. The triruthenium alkynes clusters are interesting because they acted as catalysts or catalyst precursors in hydrogenation [47], their theoretical studies[45], their biological activities as an anticancer drug[48], and they have redox centres, such as the ferrocenyl group[49].

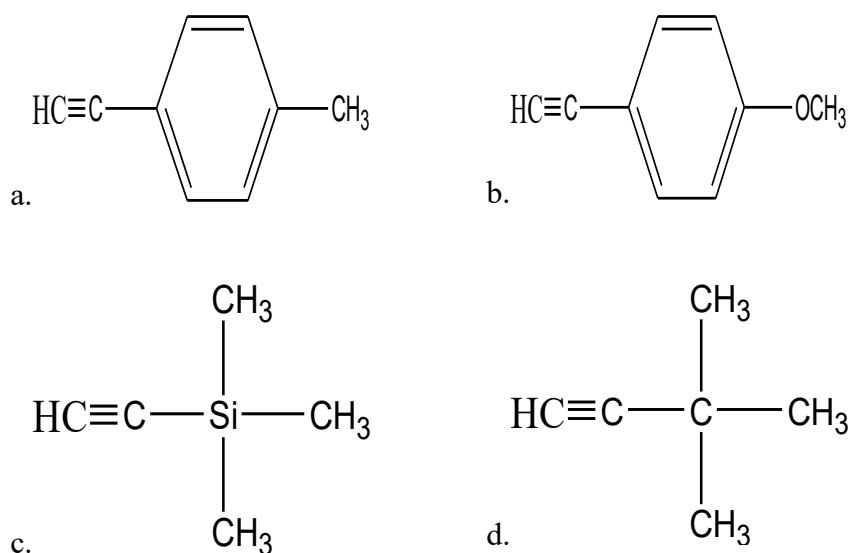
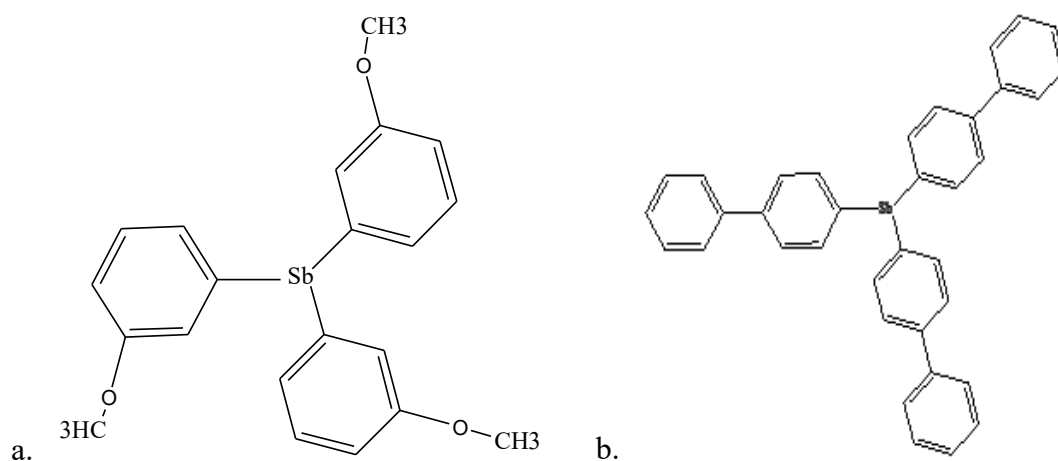


Figure 1.2 a) $\text{CH}_3\text{-4-C}_6\text{H}_5\text{C}_2\text{H}$, b) $\text{CH}_3\text{O-4-C}_6\text{H}_5\text{C}_2\text{H}$, c) $(\text{CH}_3)_3\text{SiC}_2\text{H}$, and d) $\text{HC}_2\text{C}(\text{CH}_3)_3$

1.2.4 Antimony ligands

Antimony was found as antimony trisulphide in nature. The antimony compounds is used for cosmetics. The main application for antimony metal is to be involved in some alloys; it is alloyed with lead or other metals to improve strength and hardness. Lead antimony alloy is also used for lead acid batteries plates and solder alloy. Antimony in the electronics industry is used to produce some semiconductor devices, such as diodes and infrared detectors. Antimony compounds are used to produce flame-retardant materials such as paints and glass [50]. Organometallic chemistry clusters containing transition metals and main group atoms are interesting, because they have the function of different properties of transition metals, and the main group atoms and may give rise to some unique chemistry [1]. Structural reports on carbonyl clusters containing ruthenium and antimony show a few structures in the

Cambridge Crystallographic Database [51–54]. Triruthenium carbonyl and their substituted compounds are of interest due to their catalytic and biological activities [54].



1.2.5 Objectives

1. To synthesise new (P, S) and antimony ligands and study the ligands' ability to act as bidentate and reactivity towards $\text{Ru}_3(\text{CO})_{12}$, $\text{Os}_3(\text{CO})_{12}$, and $\text{Ru}_3(\text{CO})_{10}(\text{LL})$.
2. To synthesise new complexes of triruthenium and triosmium clusters containing alkyne, phosphorus and sulphur containing, and antimony ligands
3. To characterise all new compounds through various analytical methods including infrared spectroscopy (IR), nuclear magnetic resonance (NMR), CHN analysis, X-ray diffraction (XRD) and determine the molecular structures of new metal cluster

complexes. In addition, a study reactivity or biological activities of these compounds will be performed.

1.2.6 Scope of the present investigation

This study is on the synthesis of new compounds by substituting carbonyl ligand in $\text{Ru}_3(\text{CO})_{12}$ with (P, S), alkyne, and antimony ligands and $\text{Os}_3(\text{CO})_{12}$ with (P, S) ligands. Also, compounds of the type $\text{Ru}_3(\text{CO})_{10}(\text{LL})$ [where LL= (dppm), (dpam), (dppe), (dppf), (dotpm), and (dpae) were synthesized.

Two sulphur containing phosphines ligands were chosen; (4-(methylthio)phenyl)diphenyl phosphino, $\text{Ph}_2\text{P}(\text{C}_6\text{H}_4)\text{SCH}_3$ and diphenyl (phenylthiomethyl) phosphine, $\text{Ph}_2\text{PCH}_2\text{SPh}$ to study the ligands' ability to act as bidentate and their reactivities towards $\text{Ru}_3(\text{CO})_{12}$ and $\text{Os}_3(\text{CO})_{12}$.

Four alkyne ligands were used; (trimethylsilyl)acetylene, $(\text{CH}_3)_3\text{SiC}_2\text{H}$, tertbutylacetylene, $\text{HC}_2\text{C}(\text{CH}_3)_3$, *paratolyl*acetylene, $\text{CH}_3\text{-4-C}_6\text{H}_5\text{C}_2\text{H}$, and *paramethoxy phenyl*acetylene, $\text{CH}_3\text{O-4-C}_6\text{H}_5\text{C}_2\text{H}$ to study the reactivities of these ligands towards $\text{Ru}_3(\text{CO})_{10}(\text{LL})$ compounds and synthesize acetylene clusters of type $\text{HRu}_3(\text{CO})_7(\text{LL})(\text{C}_2\text{R})$.

Two new and novel antimony ligands were synthesised, namely, tris *meta* methoxyphenylantimony, $\text{Sb}(\text{C}_6\text{H}_4\text{-3-OCH}_3)_3$ and tris biphenylantimony, $\text{Sb}(\text{C}_{12}\text{H}_9)_3$.

A study of their reactivities towards $\text{Ru}_3(\text{CO})_{12}$, $\text{Ru}_3(\text{CO})_{10}(\text{dppm})$, and $\text{Ru}_3(\text{CO})_{10}(\text{dpae})$ compounds.

All the new synthesised cluster complexes were characterised using infrared spectroscopy (IR), nuclear magnetic resonance spectroscopy (NMR), CHN analysis and single crystal X-ray diffraction (XRD). IR is one of the first spectroscopic techniques applied to the study of carbonyl clusters with its capability in identifying carbonyl stretching and other functional groups. CHN analysis is used to determine the exact composition of carbon, hydrogen, and nitrogen elements within the compound. NMR is spectroscopic technique determining the chemical shift of ^1H , ^{13}C , and ^{31}P nuclei in the cluster complexes. A single crystal X-ray diffraction (XRD) study is required to obtain more detailed and accurate information about the atomic molecular and geometric parameters. It is clear that these studies enabled us to make a detailed comparison of the molecular geometries which resulted from the substitution of CO by (P, S), acetylene, and antimony ligands. Furthermore, they allow the exploration of the chemical properties of the novel clusters. Moreover, the establishment of such novel clusters presents new opportunities in both fundamental science and its application.

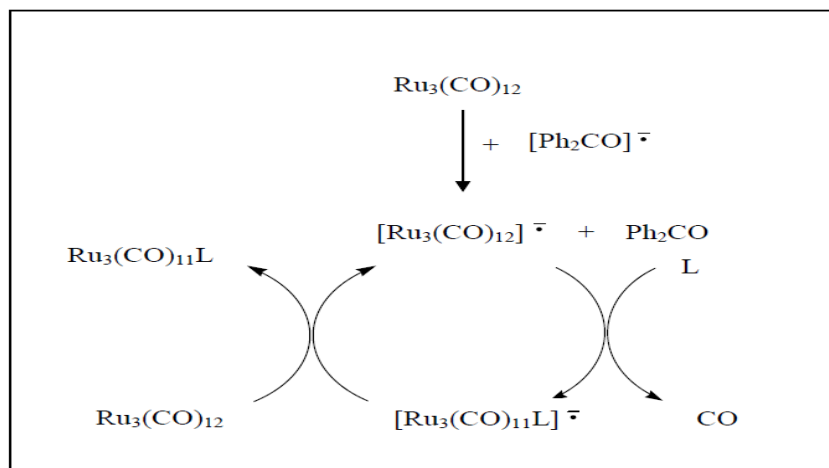
CHAPTER 2

LITERATURE REVIEW

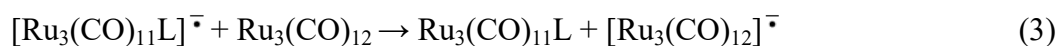
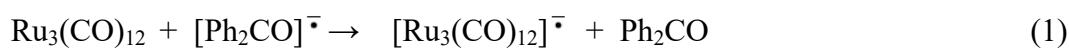
2.1 Carbonyl substitution

Triruthenium dodecacarbonyl reacts with phosphorus, arsenic, and antimony ligands through various methods of substitution reactions. The initial studies on $\text{Ru}_3(\text{CO})_{12}$ substituted by PPh_3 afforded $[\text{Ru}_3(\text{CO})_9(\text{PPh}_3)_3]$ using the thermal method [55]. Candlin and Shortland studied the thermal substitution of CO by PPh_3 , $\text{PPh}_2(\text{C}_2\text{H}_5)$, $\text{PPh}(\text{C}_2\text{H}_5)_2$, $\text{P}(\text{C}_4\text{H}_9)_3$, and $\text{P}(\text{OPh})_3$ in $\text{Ru}_3(\text{CO})_{12}$. These reactions were reported to give only the tris-substituted complexes with no proof of the mono- or bis-substituted species [29,56].

Study on reactions of $\text{Pt}(\text{PPh}_3)_4$, or $\text{Pt}(\text{PPh}_3)_2(\text{olefin})$ with $\text{Ru}_3(\text{CO})_{12}$ and $\text{Os}_3(\text{CO})_{12}$ where different types of expected products were reported [57]. These reactions are also excellent sources of the clusters type $\text{Ru}_3(\text{CO})_{12-n} \text{L}_n$ ($n = 1, 2,$ or 3) [57]. Bruce et al. and Rieger et al. reported that CO substitution can be catalysed by Na/benzophenone radical anion [55,58,59]. Bruce and co-workers had introduced new methods to activate $\text{Ru}_3(\text{CO})_{12}$ using sodium benzophenone ketyl radical anion to encourage specific carbonyl substitution of the metal clusters. This substitution involves an electron transfer catalysed (ETC) process. The proposed mechanism of the electron transfer process with $\text{Ru}_3(\text{CO})_{12}$ is shown in following Scheme [28,29,55,60].



Scheme 2.1 catalytic cycle of benzophenone ketyl anion reaction mechanism [60].



The radical anion $[\text{Ru}_3(\text{CO})_{12}]^{\cdot-}$, becomes a reactive species, where the extra electron is in antibonding orbital, leading to a weakened Ru-Ru metal bond. This bond is cleaved, leaving a 17 electron centre, which will be attacked by the ligand resulting in the elimination of CO. The reformation of the metal-metal bond yields a substituted radical anion $[\text{Ru}_3(\text{CO})_{11}\text{L}]^{\cdot-}$, which transfers an electron to an unsubstituted ruthenium cluster to continue the catalytic cycle. The requirements for this reaction to occur are that the cluster carbonyl needs to reduce without fragmentation, and the resulting radical has to have a long enough lifetime to allow for substitution. The substituting ligand must be a higher Lewis

base than the carbonyl ligand. Secondly, the ligand must not be reduced by the diphenylketyl radical anion. When these conditions are met, this method allows for short reaction times, mild conditions, high product yields and also leads to the isolation of many complexes that were previously difficult to obtain. These techniques provide a convenient platform for preparation of a variety of substitution products. For example, the utility of this technique was shown in synthesising some mono, di- and tri-substituted cluster complexes of $\text{Ru}_3(\text{CO})_{12}$ [29].

Bis(triphenylphosphine)iminium (acetate/cyanide) $[\text{PPN}][\text{OAc}]$ or $[\text{PPN}][\text{CN}]$ activate $\text{Ru}_3(\text{CO})_{12}$ towards specific CO substitution. Lavinge and Kaesz discovered that the catalytic amount of $[\text{PPN}][\text{OAc}]$ in the reaction would support substitution by tertiary phosphine such as PPh_3 , dppm, and dppe [61]. Cullen et al. also, studied the catalytic reaction for dppf using $[\text{PPN}][\text{OAc}]$ [62]. Therefore, other $[\text{PPN}]^+$ salts show varying degrees of activities, and rates of ligand substitution in $\text{Ru}_3(\text{CO})_{12}$ enhanced by the addition of methoxide ion, which formed the labile methoxycarbonyl complex $[\text{Ru}_3(\text{CO}_2\text{Me})(\text{CO})_{11}]$ [63]. These methods reveal that such complexes have a higher reactivity towards nucleophilic reagents, undergoing carbonyl substitution reactions and nucleophilic additions to coordinated CO ligands under very mild conditions [64].

Trimethylamine N-oxide, Me_3NO activates the replacement of carbonyl in $\text{Ru}_3(\text{CO})_{12}$ in the presence of a labile ligand such as acetonitrile MeCN, which is

replaced very fast. These complexes $[\text{Ru}_3(\text{CO})_{11}(\text{MeCN})]$ and $[\text{Ru}_3(\text{CO})_{10}(\text{MeCN})_2]$ were prepared at low temperature [65]. The use of Me_3NO to remove co-ordinated carbon monoxide was first reported by Shvo and Hazum [66].

The photochemical initiator is the most interesting applications of these photogenerated reducing agents. The electron transfer (ETC) catalysed carbonyl substitution of $\text{Ru}_3(\text{CO})_{12}$ produces $[\text{Ru}_3(\text{CO})_{11}(\text{PMe}_2\text{Ph})] + \text{CO}$ [67]. In 1986 a comprehensive investigation of the medium, ligand, and wavelength effects on the quantum yields and flash photolysis kinetics for the photo-fragmentation and photosubstitution reactions of the $\text{Ru}_3(\text{CO})_{12}$ was reported [68]. For example studied of the substituted clusters of type $\text{Ru}_3(\text{CO})_{12-n} \text{L}_n$, ($\text{L} = \text{P}(\text{OCH}_3)_3$, PPh_3 , $\text{P}(\text{p-tolyl})_3$, or $\text{P}(\text{O}(\text{o-tolyl}))_3$). These results were interpreted regarding the following model for $\text{Ru}_3(\text{CO})_{12}$ photochemistry. Photo-fragmentation (e.g., $\text{Ru}_3(\text{CO})_{12} + 3\text{L} \rightarrow 3\text{Ru}(\text{CO})_4\text{L}$) occurs mainly from the lowest energy excited state and proceeds via an intermediate isomeric to $\text{Ru}_3(\text{CO})_{12}$ but not a diradical. It was proposed to have one coordinatively unsaturated ruthenium centre trappable by a two-electron donor, i.e., L, to produce a second intermediate $\text{Ru}_3(\text{CO})_{12}\text{L}$ which is the precursor to the photo-fragmentation products. This reaction (e.g. $\text{Ru}_3(\text{CO})_{12} + \text{L} \rightarrow [\text{Ru}_3(\text{CO})_{11}\text{L}] + \text{CO}$) was proposed to occur largely from higher energy states through CO dissociation to produce the unsaturated intermediate $\text{Ru}_3(\text{CO})_{11}$. Moreover, the photolysis was dependent on

the nature of L, and photolysis studies established the reactivity of this species with different L to follow the order $\text{CO} > \text{P}(\text{OCH}_3)_3 > \text{PPh}_3$ [68].

$\text{Os}_3(\text{CO})_{12}$ is more stable than $\text{Ru}_3(\text{CO})_{12}$ and many reactions can be carried out without any change of nuclearity. Os_3 systems are often quite stable to air and heat and easily crystallised [26]. Thermal reactions involving $\text{Os}_3(\text{CO})_{12}$ and phosphines or arsines ligands produced a mixture of mono-, di-, and tri-substituted of triosmium clusters, by controlling the stoichiometry, a good yield of the product can be obtained in using chromatography separation. Chemical activation of $\text{Os}_3(\text{CO})_{12}$ can be carried out with Na/benzophenone radical anion [60]. Also, chemical activation of $\text{Os}_3(\text{CO})_{12}$ with Me_3NO , which was first introduced by Shvo and Hazum removing CO groups through the formation of CO_2 [66]. Since phosphine and arsine are also susceptible to oxidation by Me_3NO , the direct reaction of $\text{Os}_3(\text{CO})_{12}$ with phosphine/arsine in the presence of Me_3NO was reported. Substitution of $\text{Os}_3(\text{CO})_{12}$ derivatives containing labile ligands is the most useful method for preparing mono- and di-substituted phosphines derivatives. Activation of $\text{Os}_3(\text{CO})_{12}$ by Me_3NO in the presence of a labile ligand such as MeCN, has been used to prepare $[\text{Os}_3(\text{CO})_{11}(\text{MeCN})]$ and $[\text{Os}_3(\text{CO})_{10}(\text{MeCN})_2]$ [42]. Other chemical activations include the use of $\text{Pt}(\text{PPh}_3)_4$ and the complexes $[\text{Os}_3(\text{CO})_{12-n}\text{L}_n]$, produced from reactions with $\text{Os}_3(\text{CO})_{12}$ [57,60]. Na/benzophenone radical anion was found to catalyse the substitution of phosphine or arsine on $\text{Os}_3(\text{CO})_{12}$. Substitution of $\text{Os}_3(\text{CO})_{12}$ derivatives containing labile ligands is a useful method for preparing mono- and di-

substituted derivatives. Arsines and phosphines react with these derivatives with great specificity [60].

2.2 Bidentate ligands with $\text{Ru}_3(\text{CO})_{12}$

The chemical reactions of diphosphine and diarsine bidentate ligands with $\text{Ru}_3(\text{CO})_{12}$ started in 1970 and were studied by Cullen and Harbourne. They reported the reactions between $\text{Ru}_3(\text{CO})_{12}$ with the fluorocarbon-bridged ligands, ffars, ffos, and $f_6\text{fos}$ respectively [69]. Since the initial studies, the substitution chemistry and subsequent reactivities and reaction mechanisms of the type $[\text{Ru}_3(\text{LL})(\text{CO})_{10}]$ and $[\text{Ru}_3(\text{LL})_2(\text{CO})_8]$ have been studied extensively.

The bidentate ligands have the potential to bind to a metal centre by chelating a single ruthenium atom within the cluster, by bridging a cluster edge and binding two ruthenium atoms, or by acting as a monodentate ligand with one free atom. In 1977, Cotton and Hanson first reported the synthesis of $[\text{Ru}_3(\text{CO})_{10}(\text{dppm})]$ from the reaction between $\text{Ru}_3(\text{CO})_{12}$ and dppm refluxed at 50°C for 36 hours [70]. $\text{Ru}_3(\text{CO})_{10}(\text{dppm})$ complex was confirmed by the characteristic pattern of the carbonyl stretching frequencies for disubstituted complexes. Later, Bruce and co-workers reported the synthesis of $[\text{Ru}_3(\text{CO})_{10}(\text{dppm})]$ at 91% yield using sodium benzophenone ketyl radical [55].

The X-ray structure afforded for $[\text{Ru}_3(\text{CO})_{10}(\text{dppm})]$ reported by Coleman and co-workers in 15% yield [71]. The interesting abnormality found in this structure was